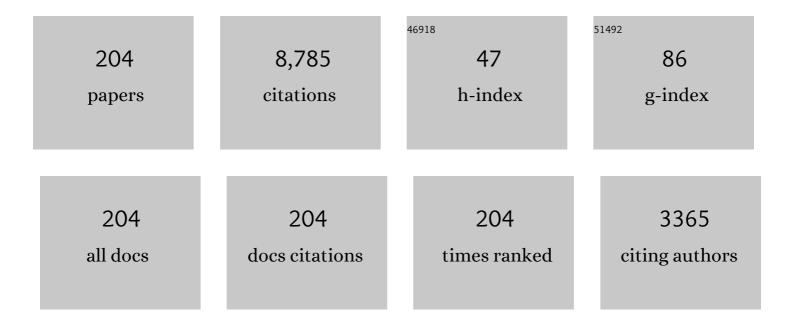
## Giulio Del Zanna

List of Publications by Year in descending order

Source: https://exaly.com/author-pdf/4370829/publications.pdf Version: 2024-02-01



#	Article	IF	CITATIONS
1	CHIANTI—An Atomic Database for Emission Lines. VII. New Data for Xâ€Rays and Other Improvements. Astrophysical Journal, Supplement Series, 2006, 162, 261-280.	3.0	404
2	CHIANTI—AN ATOMIC DATABASE FOR EMISSION LINES. XIII. SOFT X-RAY IMPROVEMENTS AND OTHER CHANGES. Astrophysical Journal, 2013, 763, 86.	1.6	401
3	CHIANTI $\hat{a} \in \hat{a}$ an atomic database for emission lines. Astronomy and Astrophysics, 2009, 498, 915-929.	2.1	379
4	CHIANTI – An atomic database for emission lines. Version 8. Astronomy and Astrophysics, 2015, 582, A56.	2.1	372
5	SDO/AIA response to coronal hole, quiet Sun, active region, and flare plasma. Astronomy and Astrophysics, 2010, 521, A21.	2.1	323
6	CHIANTI—AN ATOMIC DATABASE FOR EMISSION LINES. XII. VERSION 7 OF THE DATABASE. Astrophysical Journal, 2012, 744, 99.	1.6	278
7	CHIANTI—An Atomic Database for Emission Lines. VI. Proton Rates and Other Improvements. Astrophysical Journal, Supplement Series, 2003, 144, 135-152.	3.0	261
8	CHIANTI—An Atomic Database for Emission Lines. XV. Version 9, Improvements for the X-Ray Satellite Lines. Astrophysical Journal, Supplement Series, 2019, 241, 22.	3.0	182
9	CHIANTI—An Atomic Database for Emission Lines. XVI. Version 10, Further Extensions. Astrophysical Journal, 2021, 909, 38.	1.6	173
10	CHIANTI—An Atomic Database for Emission Lines. IV. Extension to Xâ€Ray Wavelengths. Astrophysical Journal, Supplement Series, 2001, 134, 331-354.	3.0	170
11	Solar active regions: SOHO/CDS and TRACE observations ofÂquiescentÂcoronal loops. Astronomy and Astrophysics, 2003, 406, 1089-1103.	2.1	169
12	Solar UV and X-ray spectral diagnostics. Living Reviews in Solar Physics, 2018, 15, 5.	7.8	158
13	Flows in active region loops observed by Hinode EIS. Astronomy and Astrophysics, 2008, 481, L49-L52.	2.1	137
14	The multi-thermal emission in solar active regions. Astronomy and Astrophysics, 2013, 558, A73.	2.1	137
15	Solar minimum streamer densities and temperatures using Whole Sun Month coordinated data sets. Journal of Geophysical Research, 1999, 104, 9691-9699.	3.3	132
16	The Structure and Evolution of a Sigmoidal Active Region. Astrophysical Journal, 2002, 574, 1021-1038.	1.6	122
17	The virtual atomic and molecular data centre (VAMDC) consortium. Journal of Physics B: Atomic, Molecular and Optical Physics, 2016, 49, 074003.	0.6	120
18	ACTIVE REGION LOOPS: <i>HINODE</i> /EXTREME-ULTRAVIOLET IMAGING SPECTROMETER OBSERVATIONS. Astrophysical Journal, 2009, 694, 1256-1265.	1.6	119

#	Article	IF	CITATIONS
19	SDO AIA and Hinode EIS observations of "warm―loops. Astronomy and Astrophysics, 2011, 535, A46.	2.1	116
20	SLIPPING MAGNETIC RECONNECTION DURING AN X-CLASS SOLAR FLARE OBSERVED BY <i>SDO</i> /AIA. Astrophysical Journal, 2014, 784, 144.	1.6	114
21	Spectroscopic diagnostics of stellar transition regions and coronae in the XUV: AU Mic in quiescence. Astronomy and Astrophysics, 2002, 385, 968-985.	2.1	96
22	Benchmarking atomic data for astrophysics: \$ion{Fe}{x}\$. Astronomy and Astrophysics, 2004, 422, 731-749.	2.1	95
23	Global maps of the magnetic field in the solar corona. Science, 2020, 369, 694-697.	6.0	92
24	A single picture for solar coronal outflows and radio noise storms. Astronomy and Astrophysics, 2011, 526, A137.	2.1	84
25	A revised radiometric calibration for the Hinode/EIS instrument. Astronomy and Astrophysics, 2013, 555, A47.	2.1	84
26	Magnetic flux cancellation associated with a recurring solar jet observed with <i>Hinode</i> , <i>RHESSI</i> , and <i>STEREO</i> /EUVI. Astronomy and Astrophysics, 2008, 491, 279-288.	2.1	83
27	The Solar Orbiter SPICE instrument. Astronomy and Astrophysics, 2020, 642, A14.	2.1	82
28	On-Orbit Degradation of Solar Instruments. Solar Physics, 2013, 288, 389-434.	1.0	80
29	Electron density and temperature of the lower solar corona. Journal of Geophysical Research, 1999, 104, 9709-9720.	3.3	78
30	SIMULTANEOUS IRIS AND HINODE/EIS OBSERVATIONS AND MODELING OF THE 2014 OCTOBER 27 X2.0ÂCLASS FLARE. Astrophysical Journal, 2016, 816, 89.	1.6	70
31	Benchmarking atomic data for astrophysics: Fe XII. Astronomy and Astrophysics, 2005, 433, 731-744.	2.1	70
32	Achievements of Hinode in the first eleven years. Publication of the Astronomical Society of Japan, 2019, 71, .	1.0	69
33	The Elephant's Trunk: Spectroscopic diagnostics applied to SOHO/CDS observations of the August 1996 equatorial coronal hole. Journal of Geophysical Research, 1999, 104, 9753-9766.	3.3	68
34	Benchmarking atomic data for the CHIANTI atomic database: coronal lines observed by Hinode EIS. Astronomy and Astrophysics, 2012, 537, A38.	2.1	60
35	Nonequilibrium Processes in the Solar Corona, Transition Region, Flares, and Solar Wind (Invited) Tj ETQq1 1 0.784	4314 rgBT 1.0	Overlock
36	JOINT HIGH TEMPERATURE OBSERVATION OF A SMALL C6.5 SOLAR FLARE WITH IRIS/EIS/AIA. Astrophysical Journal, 2015, 803, 84.	1.6	59

#	Article	IF	CITATIONS
37	Spectroscopic characteristics of polar plumes. Astronomy and Astrophysics, 2003, 398, 743-761.	2.1	58
38	Title is missing!. Solar Physics, 1997, 170, 143-161.	1.0	56
39	Multiwavelength study of 20 jets that emanate from the periphery of active regions. Astronomy and Astrophysics, 2016, 589, A79.	2.1	53
40	A Decade with VAMDC: Results and Ambitions. Atoms, 2020, 8, 76.	0.7	53
41	Elemental abundances and temperatures of quiescent solar active region cores from X-ray observations. Astronomy and Astrophysics, 2014, 565, A14.	2.1	52
42	Atomic data from the IRON Project. Astronomy and Astrophysics, 2005, 433, 717-730.	2.1	51
43	The 22 May 2007 B-class flare: new insights from <i>Hinode</i> observations. Astronomy and Astrophysics, 2011, 526, A1.	2.1	51
44	SOLAR TRANSITION REGION LINES OBSERVED BY THE <i>INTERFACE REGION IMAGING SPECTROGRAPH</i> : DIAGNOSTICS FOR THE O IV AND Si IV LINES. Astrophysical Journal Letters, 2014, 780, L12.	3.0	51
45	Solar EUV spectroscopic observations with SOHO/CDS. Astronomy and Astrophysics, 2001, 379, 708-734.	2.1	49
46	A Multi-Wavelength Study of the Compact M1 Flare on October 22, 2002. Solar Physics, 2006, 234, 95-113.	1.0	49
47	Solar Coronal Lines in the Visible and Infrared: A Rough Guide. Astrophysical Journal, 2018, 852, 52.	1.6	49
48	The EUV helium spectrum in the quiet Sun: A by-product of coronal emission?. Astronomy and Astrophysics, 2003, 400, 737-752.	2.1	49
49	Benchmarking atomic data for astrophysics: a first look at the soft X-ray lines. Astronomy and Astrophysics, 2012, 546, A97.	2.1	48
50	Atomic data for astrophysics: Fe x soft X-ray lines. Astronomy and Astrophysics, 2012, 541, A90.	2.1	47
51	Propagating Disturbances in Coronal Loops: A Detailed Analysis of Propagation Speeds. Solar Physics, 2012, 279, 427-452.	1.0	47
52	Density diagnostics derived from the O iv and S iv intercombination lines observed by IRIS. Astronomy and Astrophysics, 2016, 594, A64.	2.1	46
53	Benchmarking atomic data for astrophysics: Fe VII and other cool lines observed by Hinode EIS. Astronomy and Astrophysics, 2009, 508, 501-511.	2.1	43
54	Benchmarking atomic data for astrophysics: Fe XVII EUV lines. Astronomy and Astrophysics, 2009, 508, 1517-1526.	2.1	43

#	Article	IF	CITATIONS
55	Flare lines in Hinode EIS spectra. Astronomy and Astrophysics, 2008, 481, L69-L72.	2.1	43
56	A Time-resolved Extreme-Ultraviolet Spectroscopic Study of the Quiescent and Flaring Corona of the Flare Star AU Microscopii. Astrophysical Journal, 1996, 466, 427.	1.6	43
57	Multiconfiguration Dirac-Hartree-Fock Calculations with Spectroscopic Accuracy: Applications to Astrophysics. Atoms, 2017, 5, 16.	0.7	40
58	Spectral diagnostics with the SDO EVE flare lines. Astronomy and Astrophysics, 2013, 555, A59.	2.1	39
59	Atomic data for astrophysics: Fe xii soft X-ray lines. Astronomy and Astrophysics, 2012, 543, A139.	2.1	39
60	Benchmarking atomic data for astrophysics: FeÂxi. Astronomy and Astrophysics, 2010, 514, A41.	2.1	38
61	On the consequences of a non-equilibrium ionisation balance for compact flare emission and dynamics. Astronomy and Astrophysics, 2004, 425, 287-299.	2.1	38
62	Active region moss. Astronomy and Astrophysics, 2010, 518, A42.	2.1	37
63	Solar active regions: The footpoints of 1 MK loops. Astronomy and Astrophysics, 2003, 406, L5-L8.	2.1	36
64	Benchmarking atomic data for astrophysics: Fe VIII EUV lines. Astronomy and Astrophysics, 2009, 508, 513-524.	2.1	36
65	<i>R</i> -MATRIX ELECTRON-IMPACT EXCITATION OF Fe <sup>13+</sup> AND ITS APPLICATION TO THE SOFT X-RAY AND EXTREME-ULTRAVIOLET SPECTROSCOPY OF CORONA-LIKE PLASMAS. Astrophysical Journal, Supplement Series, 2010, 190, 322-333.	3.0	36
66	Active Region Loops: Temperature Measurements as a Function of Time from JointTRACEandSOHOCDS Observations. Astrophysical Journal, 2007, 655, 598-605.	1.6	35
67	Density structure of an active region and associated moss using Hinode/EIS. Astronomy and Astrophysics, 2008, 481, L53-L56.	2.1	35
68	Hinode extreme-ultraviolet imaging spectrometer observations of a limb active region. Astronomy and Astrophysics, 2011, 525, A137.	2.1	35
69	Non-Maxwellian Analysis of the Transition-region Line Profiles Observed by the Interface Region Imaging Spectrograph. Astrophysical Journal, 2017, 842, 19.	1.6	35
70	Atomic data from the IRON project. Astronomy and Astrophysics, 2010, 514, A40.	2.1	34
71	A RECONNECTION-DRIVEN RAREFACTION WAVE MODEL FOR CORONAL OUTFLOWS. Astrophysical Journal, 2011, 743, 66.	1.6	34
72	Benchmarking atomic data for astrophysics: Fe xiii EUV lines. Astronomy and Astrophysics, 2011, 533, A12.	2.1	31

#	Article	IF	CITATIONS
73	<i>R</i> -matrix electron-impact excitation data for the Be-like iso-electronic sequence. Astronomy and Astrophysics, 2014, 566, A104.	2.1	31
74	Analysis and modelling of recurrent solar flares observed with Hinode/EIS on March 9, 2012. Astronomy and Astrophysics, 2017, 601, A39.	2.1	30
75	The evolution of the emission measure distribution in the core of an active region. Astronomy and Astrophysics, 2015, 573, A104.	2.1	30
76	Atomic data for astrophysics: Fe xiii soft X-ray lines. Astronomy and Astrophysics, 2012, 543, A144.	2.1	29
77	Atomic data for the X-ray lines of Fe viii and Fe ix. Astronomy and Astrophysics, 2012, 537, A22.	2.1	29
78	Large-scale Multiconfiguration Dirac–Hartree–Fock Calculations for Astrophysics: Cl-like Ions from Cr viii to Zn xiv. Astrophysical Journal, Supplement Series, 2020, 246, 1.	3.0	29
79	Electron-impact excitation of Be-like Mg. Astronomy and Astrophysics, 2008, 487, 1203-1208.	2.1	28
80	Signatures of the non-Maxwellian <i>κ</i> -distributions in optically thin line spectra. Astronomy and Astrophysics, 2014, 570, A124.	2.1	28
81	Energy Levels, Lifetimes, and Transition Rates for P-like Ions from Cr x to Zn xvi from Large-scale Relativistic Multiconfiguration Calculations. Astrophysical Journal, Supplement Series, 2018, 235, 27.	3.0	28
82	SDO AIA and EVE observations and modelling of solar flare loops. Astronomy and Astrophysics, 2012, 547, A25.	2.1	27
83	IMAGING AND SPECTROSCOPIC OBSERVATIONS OF A TRANSIENT CORONAL LOOP: EVIDENCE FOR THE NON-MAXWELLIAN <i>1º</i>	1.6	27
84	UNDERFLIGHT CALIBRATION OF <i>SOHO</i> /CDS AND <i>HINODE</i> /EIS WITH EUNIS-07. Astrophysical Journal, Supplement Series, 2011, 197, 32.	3.0	26
85	Atomic data for astrophysics: FeÂlX. Astronomy and Astrophysics, 2014, 565, A77.	2.1	26
86	Atomic processes for astrophysical plasmas. Journal of Physics B: Atomic, Molecular and Optical Physics, 2016, 49, 094001.	0.6	26
87	Benchmarking Atomic Data from Large-scale Multiconfiguration Dirac–Hartree–Fock Calculations for Astrophysics: S-like Ions from Cr ix to Cu xiv. Astrophysical Journal, Supplement Series, 2018, 239, 30.	3.0	26
88	The EUV spectrum of the Sun: long-term variations in the SOHO CDS NIS spectral responsivities. Astronomy and Astrophysics, 2010, 518, A49.	2.1	25
89	The EUV spectrum of the Sun: SOHO CDS NIS irradiances from 1998 until 2010. Astronomy and Astrophysics, 2011, 528, A139.	2.1	25
90	The EVE Doppler Sensitivity and Flare Observations. Solar Physics, 2011, 273, 69-80.	1.0	25

#	Article	IF	CITATIONS
91	LEMUR: Large European module for solar Ultraviolet Research. Experimental Astronomy, 2012, 34, 273-309.	1.6	25
92	<i>R</i> -matrix electron-impact excitation data for the Mg-like iso-electronic sequence. Astronomy and Astrophysics, 2014, 572, A115.	2.1	25
93	Multi-instrument observations of a failed flare eruption associated with MHD waves in a loop bundle. Astronomy and Astrophysics, 2017, 600, A37.	2.1	25
94	Atomic data from the IRON Project. Astronomy and Astrophysics, 2005, 430, 331-341.	2.1	24
95	Benchmarking atomic data for astrophysics: \$ion{Fe}{xxiii}\$. Astronomy and Astrophysics, 2005, 432, 1137-1150.	2.1	24
96	Hinode observations and 3D magnetic structure of an X-ray bright point. Astronomy and Astrophysics, 2011, 526, A134.	2.1	23
97	Spectroscopy of Very Hot Plasma in Non-flaring Parts of a Solar Limb Active Region: Spatial and Temporal Properties. Astrophysical Journal, 2017, 846, 25.	1.6	22
98	Atomic data from the IRON project. Astronomy and Astrophysics, 2006, 446, 361-366.	2.1	22
99	Benchmarking atomic data for astrophysics: Fe xviii. Astronomy and Astrophysics, 2006, 459, 307-316.	2.1	22
100	A benchmark study for CHIANTI based on RESIK solar flare spectra. Astronomy and Astrophysics, 2007, 462, 323-330.	2.1	21
101	Atomic data for astrophysics: Fe xi soft X-ray lines. Astronomy and Astrophysics, 2013, 549, A42.	2.1	21
102	Cool and hot emission in a recurring active region jet. Astronomy and Astrophysics, 2017, 606, A4.	2.1	21
103	The Gradual Phase of the X17 Flare on October 28, 2003. Solar Physics, 2006, 239, 173-191.	1.0	19
104	Nonthermal and thermal diagnostics of a solar flare observed with RESIK and RHESSI. Astronomy and Astrophysics, 2008, 488, 311-321.	2.1	19
105	OBSERVATIONS OF PLASMA UPFLOW IN A WARM LOOP WITH <i>HINODE</i> /EIS. Astrophysical Journal Letters, 2012, 754, L4.	3.0	19
106	DOPPLER SHIFTS IN ACTIVE REGION MOSS USING <i>SOHO</i> /SUMER. Astrophysical Journal, 2013, 767, 107.	1.6	19
107	Validity of the ICFT R-matrix method: Be-like Al 9+ a case study. Monthly Notices of the Royal Astronomical Society, 2015, 450, 4174-4183.	1.6	19
108	The CHIANTI atomic database. Journal of Physics B: Atomic, Molecular and Optical Physics, 2016, 49, 074009.	0.6	19

#	Article	IF	CITATIONS
109	Evolution and magnetic topology of the M 1.0 flare of October 22, 2002. Astronomy and Astrophysics, 2004, 423, 1119-1131.	2.1	19
110	Benchmarking atomic data for astrophysics: Fe XVII X-ray lines. Astronomy and Astrophysics, 2011, 536, A59.	2.1	18
111	Thermal structure of a hot non-flaring corona from Hinode/EIS. Astronomy and Astrophysics, 2014, 564, A3.	2.1	18
112	The magnetic local time distribution of energetic electrons in the radiation belt region. Journal of Geophysical Research: Space Physics, 2017, 122, 8108-8123.	0.8	18
113	The EUV spectrum of the Sun: Quiet- and active-Sun irradiances and chemical composition. Astronomy and Astrophysics, 2019, 624, A36.	2.1	18
114	Evolution of Elemental Abundances during B-Class Solar Flares: Soft X-Ray Spectral Measurements with Chandrayaan-2 XSM. Astrophysical Journal, 2021, 920, 4.	1.6	18
115	Correlation between coronal hole and quiet Sun intensities: Evidence for continuous reconnection. Astronomy and Astrophysics, 2005, 432, 341-347.	2.1	17
116	Atomic data from the IRON project. Astronomy and Astrophysics, 2007, 466, 763-770.	2.1	17
117	Incorporating Uncertainties in Atomic Data into the Analysis of Solar and Stellar Observations:ÂA Case Study in Fe xiii. Astrophysical Journal, 2018, 866, 146.	1.6	17
118	Atomic Data for Plasma Spectroscopy: The CHIANTI Database, Improvements and Challenges. Atoms, 2020, 8, 46.	0.7	17
119	Fe <scp>iii</scp> Âemission in quasars: evidence for a dense turbulent medium. Monthly Notices of the Royal Astronomical Society, 2020, 496, 2565-2576.	1.6	17
120	Electron densities in EUV coronal bright points. Astronomy and Astrophysics, 2005, 435, 1169-1172.	2.1	16
121	Temperature and density structure of a recurring active region jet. Astronomy and Astrophysics, 2017, 598, A11.	2.1	16
122	Solar microflares: a case study on temperatures and the Feâ€XVIII emission. Astronomy and Astrophysics, 2019, 628, A134.	2.1	16
123	Modelling ion populations in astrophysical plasmas: carbon in the solar transition region. Astronomy and Astrophysics, 2019, 626, A123.	2.1	16
124	Determination of the Equatorial Electron Differential Flux From Observations at Low Earth Orbit. Journal of Geophysical Research: Space Physics, 2018, 123, 9574-9596.	0.8	15
125	The EUV spectrum of the Sun: SOHO CDS NIS radiances during solar cycle 23. Astronomy and Astrophysics, 2014, 563, A26.	2.1	14
126	Predicting the COSIE-C Signal from the Outer Corona up to 3 Solar Radii. Astrophysical Journal, 2018, 865, 132.	1.6	14

#	Article	IF	CITATIONS
127	Coronal Plasma Characterization via Coordinated Infrared and Extreme Ultraviolet Observations of a Total Solar Eclipse. Astrophysical Journal, 2019, 880, 102.	1.6	14
128	Unfolding Overlapped Slitless Imaging Spectrometer Data for Extended Sources. Astrophysical Journal, 2019, 882, 12.	1.6	14
129	On the Importance of Gradients in the Lowâ€Energy Electron Phase Space Density for Relativistic Electron Acceleration. Journal of Geophysical Research: Space Physics, 2019, 124, 2628-2642.	0.8	14
130	Reconstruction of the solar EUV irradiance from 1996 to 2010 based on SOHO/EIT images. Journal of Space Weather and Space Climate, 2014, 4, A30.	1.1	13
131	Elemental composition in quiescent prominences. Astronomy and Astrophysics, 2019, 625, A52.	2.1	13
132	Plasma Diagnostics from Active Region and Quiet-Sun Spectra Observed by Hinode/EIS: Quantifying the Departures from a Maxwellian Distribution. Astrophysical Journal, 2020, 893, 34.	1.6	13
133	High Resolution Soft X-ray Spectroscopy and the Quest for the Hot (5–10 MK) Plasma in Solar Active Regions. Frontiers in Astronomy and Space Sciences, 2021, 8, .	1.1	13
134	Benchmarking atomic data for astrophysics: \$ion{Fe}{xxiv}\$. Astronomy and Astrophysics, 2006, 447, 761-768.	2.1	13
135	Relative intensity calibration of CDS-GIS detectors on SOHO using a plasma diagnostic technique. Astronomy and Astrophysics, 1999, 135, 171-185.	2.1	13
136	Sigmoidal diagnostics with SOHO/CDS. Advances in Space Research, 2002, 30, 551-556.	1.2	12
137	Benchmarking atomic data for astrophysics: Si iii. Astronomy and Astrophysics, 2015, 574, A99.	2.1	12
138	Uncertainties on atomic data. A case study: N <scp>iv</scp> . Monthly Notices of the Royal Astronomical Society, 2019, 484, 4754-4759.	1.6	12
139	Hinode EIS line widths in the quiet corona up to 1.5 <i>R</i> <sub>⊙</sub> . Astronomy and Astrophysics, 2019, 631, A163.	2.1	12
140	Effects of density on the oxygen ionization equilibrium in collisional plasmas. Monthly Notices of the Royal Astronomical Society, 2020, 497, 1443-1456.	1.6	12
141	SOHO CDS and SUMER observations of quiescent filaments andÂtheirÂinterpretation. Astronomy and Astrophysics, 2004, 420, 307-317.	2.1	12
142	Coronal Diagnostics from Narrowband Images Around 30.4 nm. Solar Physics, 2012, 279, 53-73.	1.0	11
143	Response of Hinode XRT to quiet Sun, active region and flare plasma. Astronomy and Astrophysics, 2014, 561, A20.	2.1	11
144	Atomic data for astrophysics: improved collision strengths for Fe viii. Astronomy and Astrophysics, 2014, 570, A56.	2.1	11

#	Article	IF	CITATIONS
145	Atomic data for astrophysics: Ni XII. Astronomy and Astrophysics, 2016, 585, A118.	2.1	11
146	Atomic data and density diagnostics for SÂiv. Monthly Notices of the Royal Astronomical Society, 2016, 456, 3720-3728.	1.6	11
147	Large-scale calculations of atomic level and transition properties in the aluminum isoelectronic sequence from TiÂX through KrÂXXIV, XeÂXLII, and WÂLXII. Atomic Data and Nuclear Data Tables, 2018, 120, 152-262.	0.9	11
148	<i>R</i> -matrix electron-impact excitation data for the C-like iso-electronic sequence. Astronomy and Astrophysics, 2020, 634, A7.	2.1	11
149	Linking the Sun to the Heliosphere Using Composition Data and Modelling. Space Science Reviews, 2021, 217, .	3.7	11
150	Elemental abundances of the low corona as derived from SOHO/CDS observations. AIP Conference Proceedings, 2001, , .	0.3	10
151	The solar corona in cycle 23. Advances in Space Research, 2002, 29, 361-372.	1.2	10
152	The EUV spectrum of the Sun: Irradiances during 1998–2014. Astronomy and Astrophysics, 2015, 584, A29.	2.1	10
153	EIT and TRACE responses to flare plasma. Astronomy and Astrophysics, 2006, 460, L53-L56.	2.1	10
154	Spectral diagnostic capabilities of Solar-B EIS. Advances in Space Research, 2005, 36, 1503-1511.	1.2	9
155	The EUV spectrum of the Sun: SOHO, SEM, and CDS irradiances. Astronomy and Astrophysics, 2015, 581, A25.	2.1	9
156	On the validity of the ICFT R-matrix method: FeÂxiv. Monthly Notices of the Royal Astronomical Society, 2015, 454, 2909-2917.	1.6	9
157	Importance of the completeness of the configuration interaction and close coupling expansions in <i>R</i> -matrix calculations for highly charged ions: electron-impact excitation of Fe <sup>20+</sup> . Journal of Physics B: Atomic, Molecular and Optical Physics, 2016, 49, 085203.	0.6	9
158	Exploring the damping of Alfvén waves along a long off-limb coronal loop, up to 1.4 <i>R</i> <sub>⊙</sub> . Astronomy and Astrophysics, 2019, 627, A62.	2.1	9
159	Signatures of the non-Maxwellian <i>κ</i> -distributions in optically thin line spectra. Astronomy and Astrophysics, 2019, 626, A88.	2.1	9
160	Study of the spatial association between an active region jet and a nonthermal type III radio burst. Astronomy and Astrophysics, 2019, 632, A108.	2.1	9
161	Large-scale Multiconfiguration Dirac–Hartree–Fock Calculations for Astrophysics: <i>n</i> = 4 Levels in P-like Ions from Mn xi to Ni xiv. Astrophysical Journal, Supplement Series, 2020, 247, 70.	3.0	9
162	Helium Line Emissivities in the Solar Corona. Astrophysical Journal, 2020, 898, 72.	1.6	9

#	Article	IF	CITATIONS
163	Atomic data for astrophysics: Ni XV. Astronomy and Astrophysics, 2014, 567, A18.	2.1	8
164	Solar Cell Degradation Due to Proton Belt Enhancements During Electric Orbit Raising to GEO. Space Weather, 2019, 17, 1059-1072.	1.3	8
165	Diagnostics of Non-Maxwellian Electron Distributions in Solar Active Regions from Fe xii Lines Observed by the Hinode Extreme Ultraviolet Imaging Spectrometer and Interface Region Imaging Spectrograph. Astrophysical Journal, 2022, 930, 61.	1.6	8
166	Title is missing!. Space Science Reviews, 1999, 87, 169-172.	3.7	7
167	Measurement of electric-dipole forbidden 3p and 3d level decay rates in Fe XII. Journal of Physics: Conference Series, 2008, 130, 012018.	0.3	7
	The 3s <sup>2</sup> 3p3d <sup>3</sup> F <sup>o</sup> term in the Si-like spectrum of Fe (Fe) Tj ETQq0 0 0 rgBT	/Overlock	10 Tf 50 552
168	Spectra and Oscillator Strengths for Astrophysical and Laboratory Plasmas Canadian Journal of Physics, 2011, 89, 403-412.	0.4	7
169	Resolution of the forbidden ( <i>J</i> = 0 → 0) excitation puzzle in Mg-like ions. Astronomy and Astrophysics, 2015, 577, A95.	2.1	7
170	Electron Densities in the Solar Corona Measured Simultaneously in the Extreme Ultraviolet and Infrared. Astrophysical Journal, 2021, 906, 118.	1.6	7
171	The In-Flight Performance of the SOHO/CDS Grazing Incidence Spectrometer. Solar Physics, 2007, 242, 187-211.	1.0	6
172	Modelling low charge ions in the solar atmosphere. Monthly Notices of the Royal Astronomical Society, 2021, 505, 3968-3981.	1.6	6
173	The center-to-limb variation of non-thermal velocities using IRIS Si IV. Monthly Notices of the Royal Astronomical Society, 0, , .	1.6	6
174	Flare-related Recurring Active Region Jets: Evidence for Very Hot Plasma. Solar Physics, 2018, 293, 1.	1.0	5
175	<i>R</i> -matrix electron-impact excitation data for the N-like iso-electronic sequence. Astronomy and Astrophysics, 2020, 643, A95.	2.1	5
176	Benchmarking Multiconfiguration Dirac–Hartree–Fock Calculations for Astrophysics: Si-like Ions from Cr xi to Zn xvii. Astrophysical Journal, Supplement Series, 2021, 257, 56.	3.0	5
177	Atomic data for astrophysics: Ni XI. Astronomy and Astrophysics, 2014, 566, A123.	2.1	4
178	High resolution spectropolarimetry: from Astrophysics to ECR plasmas. Journal of Instrumentation, 2018, 13, C11020-C11020.	0.5	4
179	The influence of photo-induced processes and charge transfer on carbon and oxygen in the lower solar atmosphere. Monthly Notices of the Royal Astronomical Society, 2021, 503, 1976-1986.	1.6	4
180	Future perspectives in solar hot plasma observations in the soft X-rays. Experimental Astronomy, 2021, 51, 453-474.	1.6	4

#	Article	IF	CITATIONS
181	Helium line emissivities for nebular astrophysics. Monthly Notices of the Royal Astronomical Society, 2022, 513, 1198-1209.	1.6	4
182	Stellar And Galactic Environment survey (SAGE). Experimental Astronomy, 2009, 23, 169-191.	1.6	3
183	The EUV spectral irradiance of the Sun from 1997 to date. Proceedings of the International Astronomical Union, 2009, 5, 78-80.	0.0	3
184	Scaling of collision strengths for highly-excited states of ions of the H- and He-like sequences. Astronomy and Astrophysics, 2016, 592, A135.	2.1	3
185	The high-energy Sun - probing the origins of particle acceleration on our nearest star. Experimental Astronomy, 2022, 54, 335-360.	1.6	3
186	Large-scale Multiconfiguration Dirac–Hartree–Fock Calculations for Astrophysics: C-like Ions from O iii to Mg vii. Astrophysical Journal, Supplement Series, 2022, 260, 50.	3.0	3
187	Roadmap on cosmic EUV and x-ray spectroscopy. Journal of Physics B: Atomic, Molecular and Optical Physics, 2020, 53, 092001.	0.6	2
188	Introduction of Zeeman splitting in CHIANTI. Journal of Plasma Physics, 2020, 86, .	0.7	2
189	Optimization of Radial Diffusion Coefficients for the Proton Radiation Belt During the CRRES Era. Journal of Geophysical Research: Space Physics, 2021, 126, e2020JA028486.	0.8	2
190	R-matrix electron-impact excitation data for the O-like iso-electronic sequence. Astronomy and Astrophysics, 2021, 653, A81.	2.1	2
191	The Sun as a Star. , 2013, , 87-205.		2
192	Modelling Inner Proton Belt Variability at Energies 1 to 10MeV using BASâ€₽RO. Journal of Geophysical Research: Space Physics, 0, , .	0.8	2
193	Stellar and galactic environment survey (SACE). Astrophysics and Space Science, 2009, 320, 231-238.	0.5	1
194	CHIANTI: An Atomic Database for Astrophysical Plasmas. Fusion Science and Technology, 2013, 63, 324-332.	0.6	1
195	Benchmarked atomic data for astrophysics. Proceedings of the International Astronomical Union, 2019, 15, 341-344.	0.0	1
196	Small-scale Turbulent Motion of the Plasma in a Solar Filament as the Precursor of Eruption. Astrophysical Journal, 2021, 918, 38.	1.6	1
197	Recent developments of the CHIANTI database in the X-ray wavelength range. , 2005, , .		0
198	X-ray emission from PTT stars. Advances in Space Research, 2006, 38, 1475-1481.	1.2	0

#	Article	IF	CITATIONS
199	R-matrix calculations for electron impact excitation. Journal of Physics: Conference Series, 2009, 194, 062006.	0.3	0
200	Solar plasma spectroscopy: achievements and future challenges. Astronomy and Geophysics, 2011, 52, 2.17-2.19.	0.1	0
201	Atomic data for astrophysics. Calculations, benchmarking and distribution. , 2012, , .		0
202	Advances in atomic data for plasma diagnostics. Journal of Physics: Conference Series, 2015, 635, 052035.	0.3	0
203	Completeness of the Configuration Interaction / Close Coupling expansion versus the relativistic formalism in R-matrix calculations. Journal of Physics: Conference Series, 2015, 635, 052034.	0.3	0
204	Non-periodic multilayer coatings for solar applications: advantages and future perspectives , 2021, , .		0